Pediatric Neurology 97 (2019) 30–37

Contents lists available at ScienceDirect

Pediatric Neurology

journal homepage: www.elsevier.com/locate/pnu

Original Article

Visual Function, Brain Imaging, and Physiological Factors in Children With Asymmetric Nystagmus due to Chiasmal Gliomas

Marcela Estrada, MD [a], John P. Kelly, PhD [a, b, *], Jason Wright, MD [c], James O. Phillips, PhD [a, d], Avery Weiss, MD [a, b]

[a] Department of Ophthalmology, University of Washington, Seattle, Washington
[b] Division of Ophthalmology, Roger H. Johnson Vision Clinic, Seattle Children's Hospital, Seattle, Washington
[c] Division of Radiology, Seattle Children's Hospital, Seattle, Washington
[d] Department of Otolaryngology, University of Washington School of Medicine, Seattle, Washington

ARTICLE INFO

Article history:
Received 12 September 2018
Accepted 21 March 2019
Available online 28 March 2019

Keywords:
Glioma
Asymmetric nystagmus
Vision
Brain imaging
Brain tumor

ABSTRACT

Purpose: Asymmetric nystagmus can be an important presenting sign of optic pathway gliomas in young children. We investigated the causes of asymmetric nystagmus in children with chiasmal or suprasellar optic pathway gliomas compared with children with similar optic pathway gliomas and stable gaze.
Methods: Longitudinal magnetic resonance imaging before and after treatment, age-corrected visual acuity, ocular examinations, video-oculography, visual evoked potentials, and retinal nerve fiber layer thickness were retrospectively reviewed.
Results: Twenty-two children were included (eight with asymmetric nystagmus and 14 with stable gaze). Subjects with asymmetric nystagmus presented at a younger age than those with stable gaze (2.0 vs 5.6 years; $P < 0.001$). None had neurofibromatosis type 1. Visual acuity, visual evoked potentials, nerve fiber layer, severity of optic atrophy, hydrocephalus, tumor volume, and tumor locations did not differ between those with asymmetric nystagmus and stable gaze. Asymmetric nystagmus resolved shortly after treatment, even though the average visual acuity did not improve. Changes in visual acuity or tumor volume were not different between those with asymmetric nystagmus and stable gaze after treatment. Eye movement recording from two subjects with asymmetric nystagmus revealed an asymmetric pendular-oscillation with vertical components. One subject with stable gaze developed asymmetric nystagmus with tumor growth into the rostral midbrain and associated unilateral vision loss. Another subject with tumor growth into the rostral midbrain acquired vertical saccade dysmetria.
Conclusion: We hypothesize that asymmetric nystagmus associated with optic pathway gliomas is caused by subclinical abnormalities to retinal axons that connect to gaze holding centers in the rostral midbrain. Direct compression of the rostral midbrain was a possible factor to asymmetric nystagmus in some subjects. However, many subjects with stable gaze also show midbrain compression.

Introduction

Acquired monocular, or asymmetric, nystagmus may be the presenting sign of a range of ocular or neurological disorders. The differential diagnosis of asymmetric nystagmus in young children includes spasmus nutans, retinal diseases, optic nerve hypoplasia, and intracranial masses.[1-9] Spasmus nutans is a self-limiting disorder in which young children present with asymmetric nystagmus, head bobbing, and torticollis. Documentation of normal visual acuity and a normal ocular examination distinguishes spasmus nutans from underlying retinal disease, neurological disorders,[2-7] or optic pathway gliomas (OPG).[3-5,9] Failure to document a normal ocular and neurological examination can prompt an extensive evaluation. In this study, we identified clinical factors and neural mechanisms in children who present with asymmetric nystagmus associated with suprasellar or chiasmal OPG. To better characterize the unique association of asymmetric nystagmus with

Conflicts of interest: None. John Kelly serves as a consultant to the University of Washington to maintain the quality control of Teller Acuity Cards, which are used in this study.

* Communications should be addressed to: Kelly; Division of Ophthalmology; Seattle Children's Hospital; OA.5.342, 4800 Sand Point Way NE; Seattle, WA, 98105.
E-mail address: john.kelly@seattlechildrens.org (J.P. Kelly).

https://doi.org/10.1016/j.pediatrneurol.2019.03.021
0887-8994/

gliomas, we compared findings in children with OPG and asymmetric nystagmus with those in children with OPG and stable gaze.

Methods

A retrospective review of patient records was approved by the Institutional Review Board of Seattle Children's Hospital and conformed to the requirements of the United States Health Insurance Portability and Privacy Act. Inclusion criteria consisted of (1) children with asymmetric nystagmus and an OPG on brain imaging, (2) children with OPG and stable gaze who had neuroimaging approximating dates to subjects with asymmetric nystagmus to compensate for advancements in neuroimaging, and (3) children having a complete ocular examination including visual acuity, examination of the fovea and optic nerve by direct or indirect ophthalmoscopy, ocular motility, and pattern visual evoked potentials (VEPs). Children with OPG presenting with bilateral conjugate nystagmus were excluded as all identified subjects had severe bilateral optic nerve atrophy and severe bilateral vision loss or blindness as the primary finding. Because no subject with asymmetric nystagmus had neurofibromatosis type I (NF1), children with NF1 were excluded from the stable gaze group.

The dates of neuroimaging extended from 1991 to 2013. All but two baseline scans were acquired at the Seattle Children's Hospital. Magnetic resonance images were acquired on a Siemens scanner (either 1.5 or 3.0 T). Although sequences and slice thickness varied across subjects owing to technological advancements, our analysis always included T1-weighted with and without contrast, T2-weighted, and T2 fluid-attenuated inversion recovery (FLAIR) imaging. Newer scan sequences included T1-magnetization prepared rapid acquisition gradient echo, contrast-enhanced T2 FLAIR, and constructive interference in steady state. Volumetric measurements and longitudinal comparison of 3D volumes were analyzed with 3Dslicer.[10] Each subject's magnetic resonance imaging was registered across their follow-up imaging (affine transform using BRAINS algorithm). Volumetric measurements always included T1-weighted sequences with contrast. After treatment, volumetric measurements utilized T2 FLAIR imaging if there was no residual contrast enhancement and no history of radiation treatment. The location of the mass (including cystic components) was manually segmented in 3Dslicer. The midbrain and brainstem were segmented from the inferior pulvinar to approximately cranial nerve XII. Compression of the midbrain could be evaluated by superimposing a normative midbrain[11] onto the subject's imaging in 3Dslicer. Compression of the proximal bilateral oculomotor nerves was assessed at the nerve root entry zones within the interpeduncular cistern (using high-resolution volumetric magnetization prepared rapid acquisition gradient echo or constructive interference in steady state imaging when available).

When available, peripapillary retinal nerve fiber layer (RNFL) thickness was measured by spectral domain optical coherence tomography with confocal scanning laser ophthalmoscope (OCT/SLO; Spectralis; Heidelberg Engineering, Germany). To compensate for eye movement artifacts, we report global RNFL thickness. SLO movies were acquired at 768 × 768 pixels (30 × 30° field) at 5.1 Hz and analyzed by ImageJ (http://imagej.nih.gov/ij).

Methods for assessing visual acuity and recording pattern VEPs have been described elsewhere.[12,13] Visual acuity was tested in the subject's preferred head or gaze position. To account for age effects, recognition and grating visual acuities were converted to log minimum angle of resolution (logMAR) and corrected for age.[13] VEPs were obtained from the midline occiput electrode (Oz in standard 10-20 coordinates). Two VEP systems were used and were carefully calibrated to ensure stability in signal amplitude, phase, and stimulus intensity between machines.[12] VEPs from 1991 to 2000 were recorded by a VENUS system (Neuroscientific Corp., NY; no longer manufactured). From the year 2000 onward, VEPs were recorded on a NeuroScan system (Compumedics USA, Charlotte, NC). We examined the responses to brief onset of horizontal gratings (0.5 cycles/degree; 150 ms on/500-ms blank screen), which reduce artifacts due to nystagmus.[13] VEP amplitude, latency, and signal-to-noise ratio (SNR) were analyzed by J.P.K., who was unaware of the subject's identity. Amplitude was quantified as the voltage difference between the dominant peak (greater than 80 ms) and the preceding negative peak. Latency was the time from stimulus onset to the dominant peak. SNR was calculated by an automated algorithm that analyzed phase and amplitude consistency of electroencephalography signals in the Fourier domain.[12] When available, interhemispheric asymmetry was noted if the ratio of left to right amplitude or left to right SNR differed by more than a factor of 2.0.[14]

When available, eye movements were obtained by binocular video-oculography (VOG; SensoMotoric Instruments; model 2D VOG; SMI, Berlin, Germany; ±0.5° resolution; 60 Hz sampling rate). Recording procedures have been described elsewhere.[15] Subjects binocularly viewed a 0.7° fixation target that was embedded onto a 5° visual stimulus. In this study we report gaze holding to a stationary target presented at primary gaze, saccades to horizontally or vertically stepped targets, and optokinetic nystagmus to drifting gratings (15, 30°/s). Eye movements were analyzed off-line with software (*http://faculty.washington.edu/jokelly/voganalysis*) that allowed for rejection of artifacts and subsequent filtering. The vestibulo-ocular reflex was not assessed in these young subjects.

Results

Subject data at baseline examination are summarized in Table 1. All subjects had an OPG involving the chiasmal or suprasellar region. Eight subjects had asymmetric nystagmus, and 14 subjects had stable gaze. Mean age at baseline was significantly less for those with asymmetric nystagmus compared with those with stable gaze (2.0 versus 5.6 years; $P < 0.001$). For those with asymmetric nystagmus, six subjects presented to medical attention with acquired asymmetric nystagmus, whereas the remaining two patients presented with failure to thrive and then subsequently were diagnosed with asymmetric nystagmus by a pediatric ophthalmologist. For the stable gaze group, presenting signs were progressive headaches with vomiting or strabismus (n = 7), failure to thrive (n = 2), precocious puberty (n = 2), progressing complex neurological deficits (hemiplegia, ataxia, and strabismus; n = 2), or incidental finding of a glioma on a computed tomographic scan for head trauma (n = 1). Biopsies in 15 subjects were consistent with either a pilocytic astrocytoma (n = 14) or a ganglioglioma (n = 1), all being World Health Organization grade 1. Duration of follow-up averaged 8.6 years (S.D. = 7.7) in the asymmetric nystagmus group and 9.3 years (S.D. = 5.4) in the stable gaze group.

Eye movements

On clinical examination, all subjects had normal ocular versions and all were able to generate saccades to eccentric targets. Except for four subjects with stable gaze, all subjects were orthotropic in primary gaze. The remaining four subjects had intermittent horizontal strabismus. No subject had clinical evidence of head nodding; anomalous head tilt; cranial nerve III, IV, or VI palsy; Duane syndrome; or internuclear ophthalmoplegia. By clinical examination, all but one subject with asymmetric nystagmus had a vertical component (Table 1). Binocular VOG recordings from subject #6 with asymmetric nystagmus are shown in Fig 1. The left eye shows a rotary pendular nystagmus of approximately 3.5 Hz

TABLE 1.
Subject Data at Baseline

#	Age/Sex	logMAR		Optic Atrophy		APD	Nystagmus	Tumor location
		OD	OS	OD	OS			
Subjects with asymmetric nystagmus								
1	0.6/F	1.23	0.50	++	−	−	Rotary, OD	C, BG, L Thal
2	0.7/F	0.65	0.10	++	++	−	Horizontal, OD > OS	C, T
3	0.8/M	0.24	0.41	−	+	−	Jerk, OS	C
4	1.8/F	0.20	0.02	++	++	−	Rotary, OD	C
5	2.4/F	1.71	0.16	++++	++	+	Vertical and torsional, OD	C
6	2.5/F	−0.30	2.20	++	+++	+	Rotatory, OS	C, L ON
7	3.0/M	OU 0.22		++	++	−	Vertical, OD	C, T
8	4.0/F	−0.04	0.96	++	++++	+	Rotary pendular, OS > OD	C
Subjects with stable gaze								
9*	1.2/M	0.08	0.08	++	+	−	Stable	C
10	1.3/M	0.15	2.50	+++	++++	+	Stable	C, T
11	2.8/M	0.79	0.31	+++	+++	+	Stable	C
12	4.0/M	3.10	0.14	++++	+++	+	Stable	C
13	5.0/F	0.10	0.18	+++	+++	+	Stable	C
14	5.3/F	1.30	1.30	+	+++	−	Stable, VGEN	C, T, B Thal.
15	5.7/F	0.30	0.30	+	+	−	Stable	C
16*	6.3/F	0.30	0.18	−	−	−	Stable	C, T
17	6.9/F	1.60	3.10	++	++++	+	Stable	C, T
18	7.1/M	0.00	0.54	++	+++	+	Stable	C, B ON, T
19	7.1/M	0.18	0.30	−	−	−	Stable	C, R Thal
20	7.6/M	0.10	0.10	−	−	−	Stable	C, T, L Thal
21	8.6/F	−0.12	0.00	++	++	+	Stable	C
22	10.0/F	0.00	0.00	−	−	−	Stable	C

Abbreviations:
APD = Afferent pupillary defect present (+) or absent (−)
BG = Basal ganglia
C = Chiasm/suprasellar
F = Female
L = Left
M = Male
OD = Right eye
ON = Optic nerve
OS = Left eye
OU = Both eyes
R = Right
T = Optic tracts
Thal = Thalamus
VGEN = Vertical gaze evoked nystagmus on upward gaze
LogMAR conversions (count fingers = 2.2, hand motion = 2.5, light perception = 2.8, no light perception = 3.1).
Optic atrophy: − = normal, + = mild temporal pallor, ++ mild atrophy, +++ = moderate atrophy, ++++ = severe atrophy.
* Developed abnormal eye movements on follow-up.

(amplitude of 5° vertical and 2.5° horizontal). The right eye also shows an intermittent pendular oscillation of 1 to 2 Hz. Asymmetric components in the vertical direction were superimposed upon random gaze shifts. Saccades and optokinetic nystagmus could not be recorded in this young child.

Two subjects in the stable gaze group acquired eye movement disorders after treatment. Subject #16 initially presented with stable gaze and was treated with chemotherapy. Her vision subsequently deteriorated, and she developed an asymmetric vertical pendular nystagmus of 2.1 Hz and 3° in the right eye (Fig 2). SLO/OCT video revealed a vertical nystagmus (approximately 3° to 5°) in the right eye and a small pendular torsional nystagmus (approximately $\leq$ 5°) in the left eye. Neuroimaging revealed subsequent enlargement of the mass with infiltration and compression of the right rostral midbrain. Before the appearance of asymmetric nystagmus, visual acuity was 20/100 right eye and 20/50 left eye without an afferent pupillary defect. Global RNFL thickness was 49 μm right eye and 55 μm left eye. Three months later when asymmetric nystagmus appeared, visual acuity declined to 20/800 in the right eye and 20/60 in the left eye. Furthermore, a mild right afferent pupillary defect was present, and there was mild progressive thinning of RFNL (global thickness 41 μm right eye and 51 μm left eye). The subject was then treated with focal beam radiation. When examined 15 months later, the asymmetric nystagmus resolved and visual acuity improved (20/60 right eye and 20/40 left eye). However, the afferent pupillary defect remained in the right eye and there was continued mild thinning of RFNL (global thickness 37 μm right eye and 46 μm left eye).

Subject #9 initially presented with stable gaze but then had complaints of reading difficulties and motion sickness following growth of his tumor. Although the subject had stable gaze holding, he had vertical saccade dysmetria with prolongation duration (Fig 3). Ocular versions were normal. Neuroimaging revealed enlargement of the mass from baseline and compression of the rostral midbrain on both sides. At the time of the acquired dysmetria of vertical saccades, there were no changes in visual acuity, RNFL thickness, or pupillary responses. He also had normal vestibular testing (chair rotation and step velocity testing in darkness) and normal optokinetic nystagmus gain. In addition, his obstructive hydrocephalus (previously requiring ventriculoperitoneal shunt) was stable.

Neuroimaging

All patients showed some level of contrast enhancement of their OPG. Hydrocephalus requiring a shunt was more common in the stable gaze group (nine of 14) versus the asymmetric nystagmus group (one of eight). Neuroimaging was available in six of eight

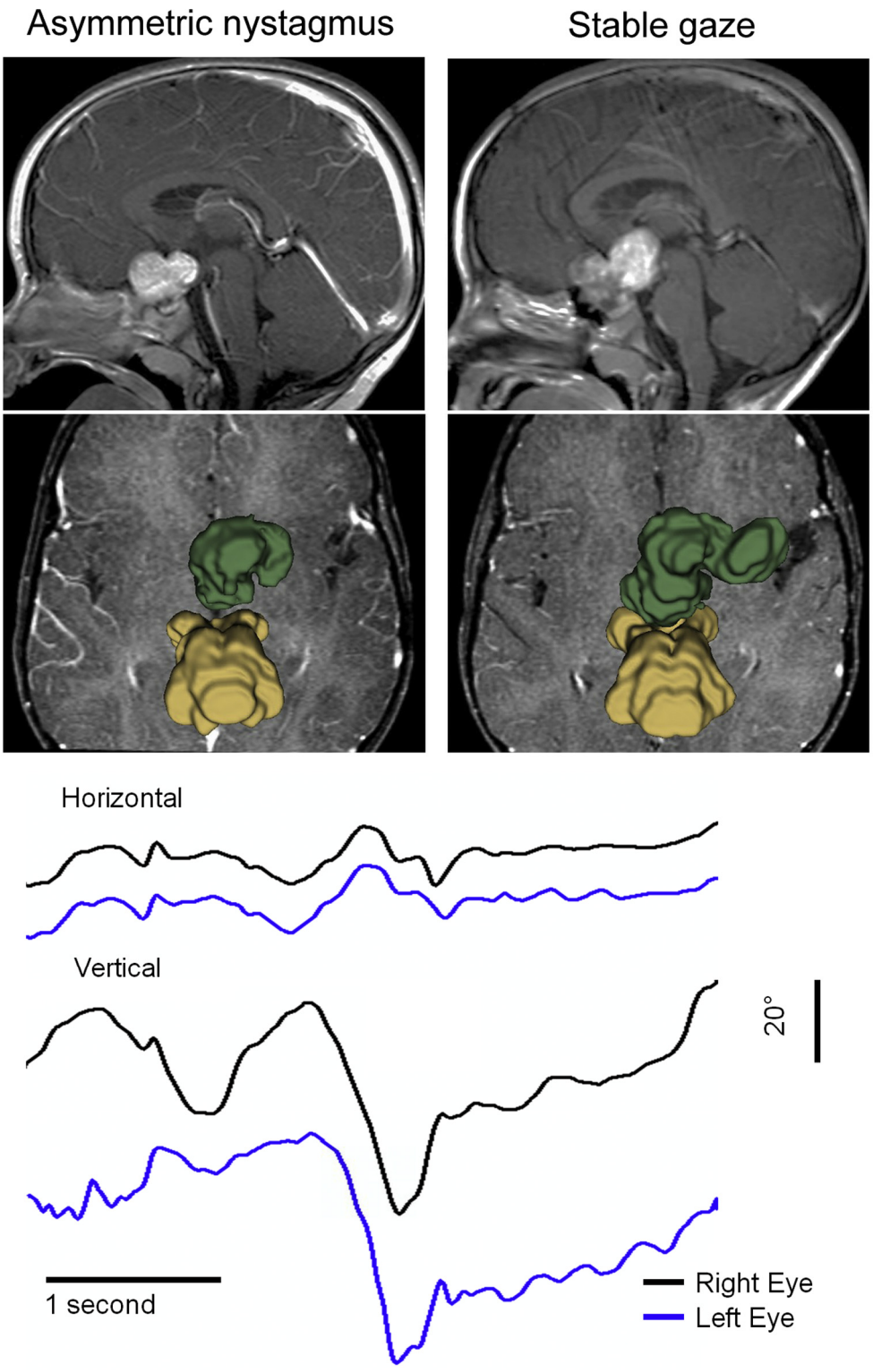

FIGURE 1. Top panel: sagittal contrast-enhanced T1-weighted images of the brain in subject #6 with asymmetric nystagmus. Imaging was performed at baseline when nystagmus was present (left side). Imaging is compared with posttreatment when asymmetric nystagmus resolved (right side). Middle panel: view from below of a three-dimensional reconstruction of the midbrain and brainstem (yellow) compared with the tumor (green). Bottom panel shows binocular video-oculography at baseline. The child is fixating a central target. Left and right eye positions are arbitrarily offset to aid comparison. For horizontal eye movements, upward and downward deflections represent rightward and leftward eye movements, respectively. For vertical eye movements, upward and downward deflections represent upward and downward eye movements, respectively. The color version of this figure is available in the online edition.

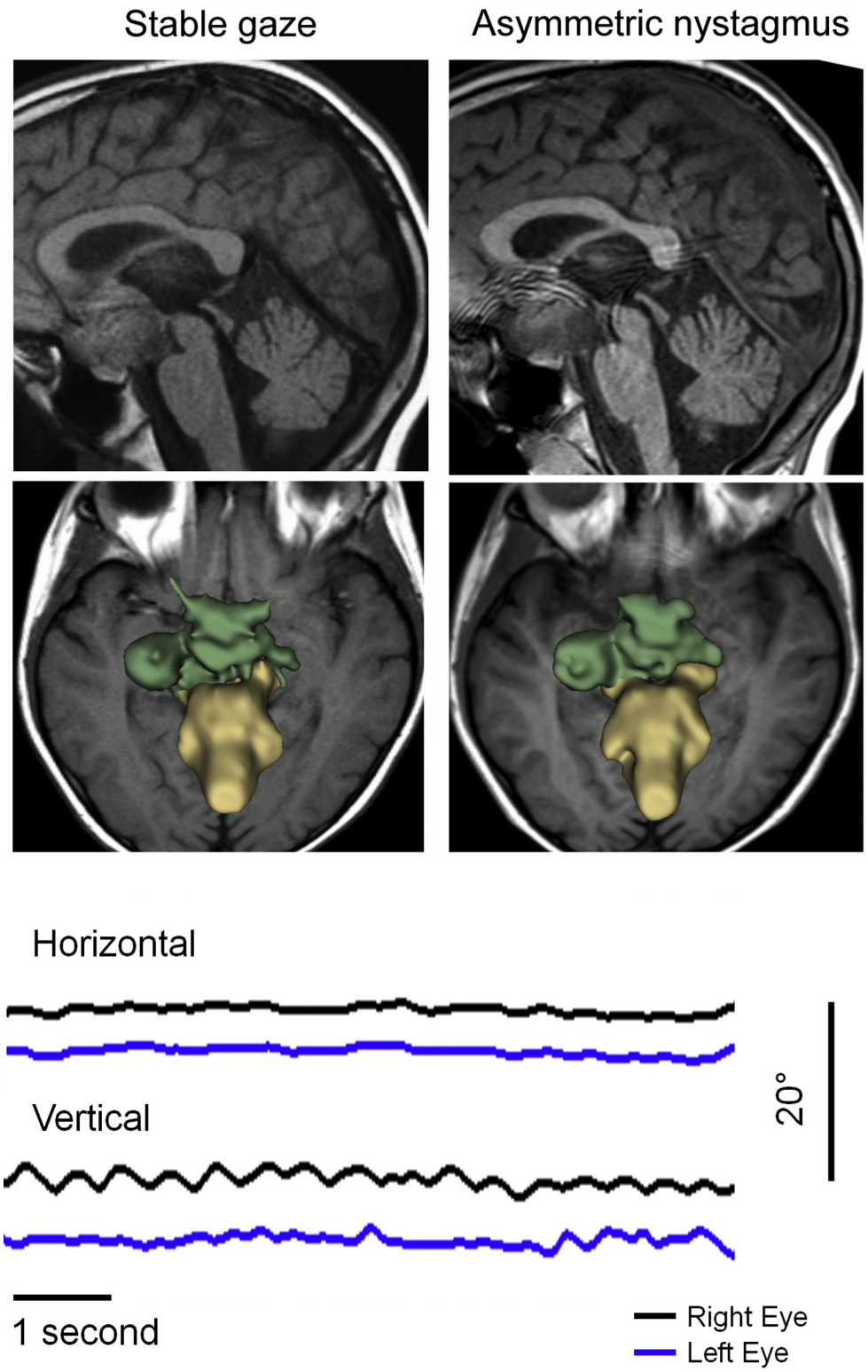

FIGURE 2. Top panel: sagittal contrast-enhanced T1-weighted images of the brain in subject #16 with acquired asymmetric nystagmus. Imaging was performed when gaze was stable before the appearance of nystagmus (left side). Imaging is compared with the time point when nystagmus was present (right side). Middle panel: view from below at a three-dimensional reconstruction of the midbrain and brainstem (yellow) compared with the tumor (green). Bottom panel: video-oculography of both eyes when nystagmus was present. For horizontal eye movements, upward and downward deflections represent rightward and leftward eye movements, respectively. For vertical eye movements, upward and downward deflections represent upward and downward eye movements, respectively. The color version of this figure is available in the online edition.

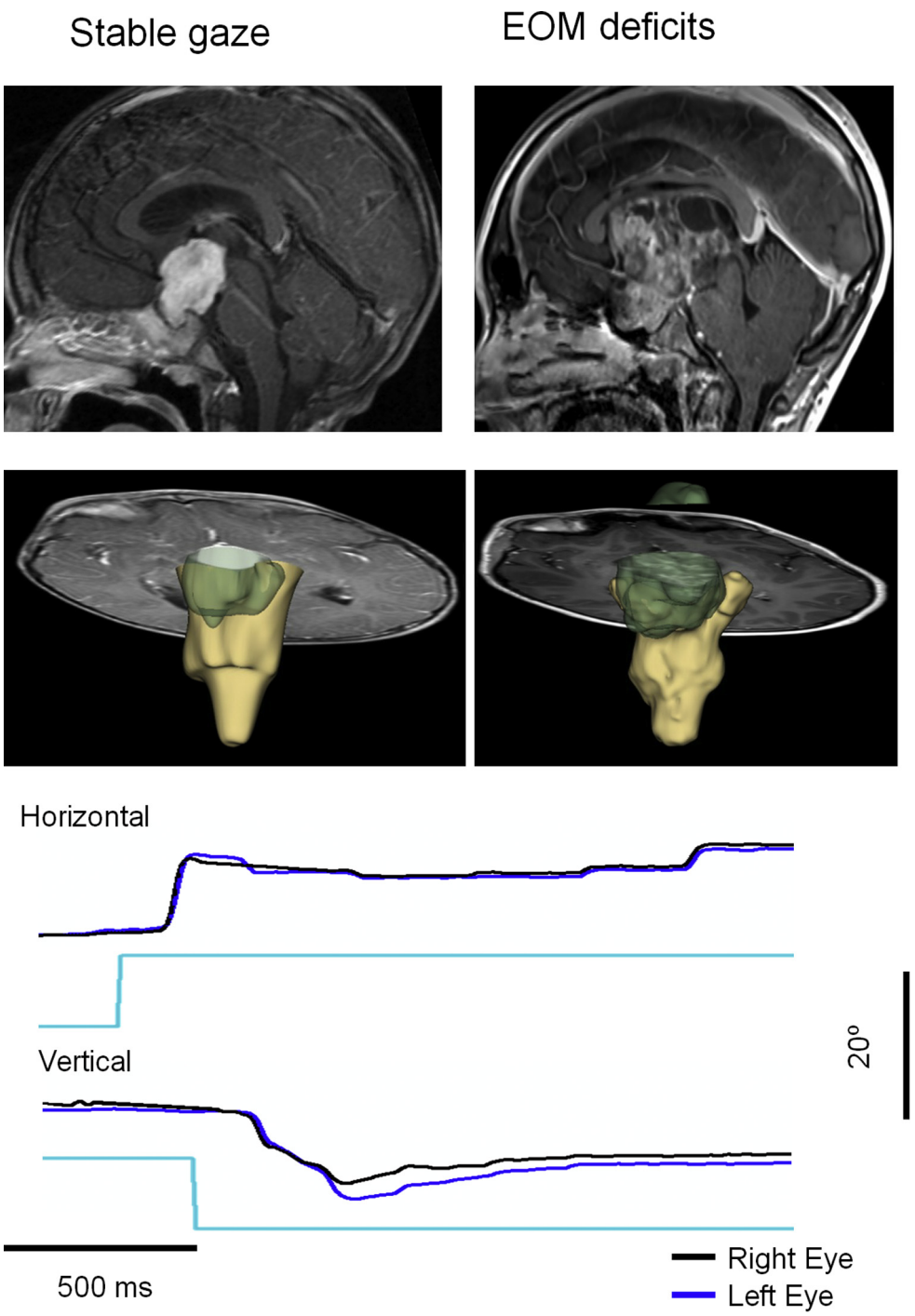

FIGURE 3. Top panel: sagittal contrast-enhanced T1-weighted images of the brain in subject #9 with acquired vertical saccade dysmetria. Imaging was performed when gaze was stable before the appearance of nystagmus (left side). Imaging is compared with the time point when nystagmus was present (right side). Middle panel: three-dimensional reconstruction of the midbrain and brainstem (yellow) compared with the tumor (green). Bottom panel: video-oculography of both eyes during horizontal or vertical saccades. For horizontal eye movements, upward and downward deflections represent rightward and leftward eye movements, respectively. For vertical eye movements, upward and downward deflections represent upward and downward eye movements, respectively. The color version of this figure is available in the online edition.

subjects in the asymmetric nystagmus group and 13 of 14 subjects in the stable gaze group. For the three subjects with missing neuroimaging, the dictated radiology report was used for analysis of general clinical variables only (i.e., the data were excluded from volumetric analysis). None of the subjects had dilation of the cerebral aqueduct or the fourth ventricle. Compression of the rostral midbrain at the level of the interpeduncular cistern was more common in the stable gaze group (eight of 13 scans) than the asymmetric nystagmus group (two of six scans). Deformation of the cranial nerve III (near the root) was similarly present in the asymmetric nystagmus group (two of six scans) and stable gaze group (five of 13 scans).

Afferent pathway

For both subject groups, the appearance of the optic nerve of the more affected eye varied from mild temporal pallor to severe atrophy (Table 1). For those with stable gaze, the optic nerves varied from normal to severely atrophic. Despite the presence of ventriculomegaly in a subset of subjects, none had papilledema and only one subject showed mild optic disk elevation. A relative afferent defect was noted in three of 10 subjects with asymmetric nystagmus and in six of 10 subjects with stable gaze. OCT of RNFL thickness was not always performed at baseline owing to age or unavailability. RNFL during follow-up was available in eight of 10 subjects with asymmetric nystagmus and nine of 14 subjects with stable gaze. For the more affected eye, there was no significant difference between groups with respect to global RNFL thickness (mean asymmetric nystagmus group = 41.3 μm; S.D. = 11.2, mean stable gaze group = 55.9 μm; S.D. = 17.8). In addition, averaged interocular difference in global RNFL was similar across asymmetric nystagmus and stable gaze groups (16.0 vs 8.3 μm, respectively; $P = 0.104$).

For the more affected eye, logMAR ranged from 0.2 to greater than 2.0 in the asymmetric nystagmus group and from 0.1 to no light perception in the stable gaze group (Mann-Whitney U-test; $P = 0.408$). VEPs (available in all subjects) were not significantly different between asymmetric nystagmus and stable gaze groups in the more affected eye with respect to amplitude, latency, or SNR ($P = 0.348$, 0.752, and 0.971, respectively). Both groups had subnormal VEP amplitudes, subnormal SNR ratios, and abnormally prolonged latencies compared with controls reported from this institution.[12] VEP interhemispheric asymmetry was similar between the asymmetric nystagmus group (three of six subjects) and stable gaze group (seven of 12 subjects).

Treatment effects and tumor volumes

All subjects with asymmetric nystagmus were initially treated with chemotherapy (carboplatin or vincristine). Treatment in those with stable gaze was by chemotherapy (n = 10), radiotherapy (n = 7), subtotal resection (n = 4), or observation only (n = 2). Nystagmus in the asymmetric nystagmus group either resolved (n = 7) or greatly improved (n = 1) after treatment with chemotherapy. Despite an improvement in nystagmus, there was no significant difference in changes in logMAR between the asymmetric nystagmus and stable gaze groups after treatment ($P = 0.26$). For the asymmetric nystagmus group, mean visual acuity in the more affected eye decreased 0.1 logMAR after treatment (range = −0.40 to +0.20; data available in six subjects). For the stable gaze group, mean visual acuity in the more affected eye decreased −0.3 logMAR after treatment (range −2.6 to 0.12; n = 14). Seven of the eight subjects in the asymmetric nystagmus group showed a response to treatment (tumor volume decreased more than 25%). Follow-up in the stable gaze group was available in 11 of 14 subjects, of which seven showed a response to treatment. At baseline, tumor volumes were similar between asymmetric nystagmus and stable gaze groups (mean 19.6 versus 27.0 cm^3, respectively; $P = 0.417$). Tumor volumes after treatment (when asymmetric nystagmus was resolved or improved) were also not different between the asymmetric nystagmus and stable gaze groups (9.8 versus 17.3 cm^3, respectively; $P = 0.182$). Figure 1 shows neuroimaging results in subject #6 with asymmetric nystagmus. At baseline, when asymmetric nystagmus was present, the mass did not contact the rostral midbrain. After treatment, asymmetric nystagmus had resolved despite enlargement of the mass into the left aspect of the sella and there was no change in visual acuity.

Discussion

This study investigated the role of multiple metrics that describe gaze holding in children who have OPG and help to elucidate the mechanisms of asymmetric nystagmus. Previous studies of asymmetric nystagmus have included subjects with a wide range of diseases. This study is unique in that subjects with asymmetric nystagmus were matched to those with stable gaze when both have with similar OPG. Visual acuity, VEP latency, VEP hemisphere symmetry, gross tumor location, hydrocephalus or ventriculomegaly, and clinical findings did not reliably discriminate children with asymmetric nystagmus from those with stable gaze. We propose two possible mechanisms that can account for asymmetric nystagmus in children with OPG involving the chiasm. One mechanism is subclinical damage to ganglion cell axons that course through the chiasm to midbrain centers that control gaze holding. The second mechanism involves compressive damage of visuomotor centers in the midbrain that control gaze holding. Each proposed mechanism is discussed in detail below.

Efferent mechanism

Most of the tumors in this study occupied the region near the oculomotor nerve root (at the interpeduncular cistern) or showed direct compression of the rostral midbrain. It is possible that specific compression of this region was a contributing factor to asymmetric nystagmus that was observed in some subjects. However, many subjects had both compression and stable gaze. No subject had clinical signs of cranial nerve palsy or showed dilation of the cerebral aqueduct or fourth ventricle, and there was no consistent evidence that hydrocephalus caused asymmetric nystagmus. In contrast, there was evidence of compression of the rostral midbrain in subjects who acquired asymmetric nystagmus (or saccade dysmetria) during follow-up. The rostral midbrain contains visuomotor centers that are implicated in optokinetic nystagmus, fine tuning of gaze control, and vertical and torsional eye movements.[16] Specifically, these tumors appear near visuomotor nuclei that include the supraoculomotor area, nucleus of the optic tract, the dorsal terminal nucleus, the rostral interstitial nucleus of the medial longitudinal fasciculus, and the interstitial nucleus of Cajal. The supraoculomotor area is involved in vergence, and its dysfunction can be associated with the difference in horizontal position between the two eyes.[17] Compressive lesions of the nucleus of the optic tract and dorsal terminal nucleus can cause a transient nystagmus because they provide direct inputs into the optokinetic nystagmus pathway.[18] Lesions of the interstitial nucleus of Cajal cause unstable vertical and torsional gaze holding, and asymmetric vertical torsional nystagmus.[19,20] Although the interstitial nucleus of Cajal plays a role in vestibular function, there was no clinical evidence of vestibular deficits or overt head tilts in this young population. Therefore one mechanism for asymmetric nystagmus might arise from abnormalities of internal feedback circuits between brainstem nuclei and cerebellum as postulated in acquired nystagmus.[21]

Afferent mechanism

The most parsimonious explanation of our data is that asymmetric nystagmus in our subjects results from an afferent mechanism. All subjects presenting with asymmetric nystagmus in the context of an OPG showed some level of optic atrophy, reduced visual acuity, abnormal VEPs, and thinner RNFL. Although these metrics of visual pathway function did not reliably differ between those with asymmetric nystagmus and stable gaze, asymmetric nystagmus was present in some subjects without any evidence of

compression of the rostral midbrain or interpeduncular cistern. This subset of subjects may have asymmetric nystagmus resulting from damage to chiasmal fibers that presumably project to oculomotor centers in the rostral midbrain (e.g., rostral interstitial nucleus of the medial longitudinal fasciculus, paramedian pontine reticular formation, or interstitial nucleus of Cajal).

Previous studies have not consistently shown that asymmetric visual acuity was a primary factor in asymmetric nystagmus.[2,5,7-9] Most studies have failed to report monocular visual acuity or objective measures of visual function and anatomy. The possibility of nystagmus-associated sensory deprivation as an etiology for asymmetric nystagmus is unlikely as there is no definitive proof that nystagmus limits visual acuity development.[13] Still, our data suggest that visual sensory abnormalities are consistently present with asymmetric nystagmus in this patient group.

Differential diagnosis

Distinguishing OPG with associated asymmetric nystagmus from spasmus nutans is important for timely treatment and prevention of morbidity from growth of this intracranial tumor. Previous studies have failed to generate clinical criteria that reliably discriminate asymmetric nystagmus associated with OPG from spasmus nutans.[2,4,22] Our subjects with asymmetric nystagmus could be distinguished from spasmus nutans by the presence of reduced visual acuity, optic nerve atrophy, and lack of head titubations. Our data are in agreement with previous studies that acquired asymmetric nystagmus can present in a relatively high percentage of chiasmal OPGs before age two years.[9]

There is only a single reported example of asymmetric nystagmus in a child with NF1-related OPG, indicating a poor association between asymmetric nystagmus and NF1.[8] As we did not observe any child with NF1-related OPG presenting with asymmetric nystagmus, we specifically excluded subjects with NF1 so that both groups could be better matched. Children with NF1-related OPG can show transient abnormal T2-weighted signals in the thalamus and brainstem,[23] which would (1) potentially confound the role oculomotor function in these subjects and (2) unlikely have a similar mechanism as a glioma.[24]

Conclusions

Although asymmetric nystagmus can be an important presenting sign of OPG previous work has not elucidated the underlying causes of the eye movement abnormality. Our study compared children with asymmetric nystagmus with those with stable gaze when both groups have similar OPGs on neuroimaging. Many factors such as visual acuity, VEP latency, VEP hemisphere symmetry, gross tumor location, ventriculomegaly, and clinical findings did not reliably discriminate children with asymmetric nystagmus from those with stable gaze. The most parsimonious explanation of our data is that asymmetric nystagmus results from damage to chiasmal fibers that project to oculomotor centers in the rostral midbrain. Furthermore, asymmetric nystagmus associated with an OPG typically resolves or improves after treatment, even if the vision does not improve.

Financial Support: Supported by an unrestricted grant from the Peter LeHaye, Barbara Anderson, and William O. Rogers Endowment Funds.

References

1. Weissman BM, Dell'Osso LF, Abel LA, Leigh RJ. Spasmus nutans. A quantitative prospective study. Arch Ophthalmol. 1987;105:525–528.
2. Farmer J, Hoyt CS. Monocular nystagmus in infancy and early childhood. Am J Ophthalmol. 1984;98:504–509.
3. Shawkat FS, Kriss A, Russel-Eggitt I, Taylor D, Harris C. Diagnosing children presenting with asymmetric pendular nystagmus. Dev Med Child Neurol. 2001;43:622–627.
4. Gottlob I, Zubcov A, Catalano RA, et al. Signs distinguishing spasmus nutans (with and without central nervous system lesions) from infantile nystagmus. Ophthalmology. 1990;97:1166–1175.
5. Newman SA, Hedges TR, Wall M, Sedwick LA. Spasmus nutans—or is it? Surv Ophthalmol. 1990;34:453–456.
6. Good WV, Koch TS, Jan JE. Monocular nystagmus caused by unilateral anterior visual-pathway disease. Dev Med Child Neurol. 1993;35:1106–1110.
7. Lopez LI, Bronstein AM, Gresty MA, Du Boulay EP, Rudge P. Clinical and MRI correlates in 27 patients with acquired pendular nystagmus. Brain. 1996;119:465–472.
8. Kiblinger GD, Wallace BS, Hines M, Siatkowski RM. Spasmus nutans-like nystagmus is often associated with underlying ocular, intracranial, or systemic abnormalities. J Neuroophthalmol. 2007;27:118–122.
9. Toledano H, Muhsinoglu O, Luckman J, Goldenberg-Cohen N, Michowiz S. Acquired nystagmus as the initial presenting sign of chiasmal glioma in young children. Eur J Paediatr Neurol. 2015;19:694–700.
10. Fedorov A, Beichel R, Kalpathy-Cramer J, et al. 3D slicer as an image computing platform for the quantitative imaging network. Magn Reson Imaging. 2012;30:1323–1341.
11. Richards JE, Sanchez C, Phillips-Meek M, Xie W. A database of age-appropriate average MRI templates. Neuroimage. 2016;124:1254–1259.
12. Kelly JP, Darvas F, Weiss AH. Waveform variance and latency jitter of the visual evoked potential in childhood. Doc Ophthalmol. 2014;128:1–12.
13. Kelly JP, Phillips JO, Weiss AH. Does eye velocity due to infantile nystagmus deprive visual acuity development? J AAPOS. 2018;22:50–55.
14. Kelly JP, Weiss AH. Comparison of pattern visual-evoked potentials to perimetry in the detection of visual loss in children with optic pathway gliomas. J AAPOS. 2006;10:298–306.
15. Weiss AH, Kelly JP, Phillips JO. Relationship of slow-phase velocity to visual acuity in infantile nystagmus associated with albinism. J AAPOS. 2011;15:33–39.
16. Giolli RA, Blanks RH, Lui F. The accessory optic system: basic organization with an update on connectivity, neurochemistry, and function. Prog Brain Res. 2006;151:407–440.
17. Das VE. Responses of cells in the midbrain near-response area in monkeys with strabismus. Invest Ophthalmol Vis Sci. 2012;53:3858–3864.
18. Schiff D, Cohen B, Büttner-Ennever J, Matsuo V. Effects of lesions of the nucleus of the optic tract on optokinetic nystagmus and after-nystagmus in the monkey. Exp Brain Res. 1990;79:225–239.
19. Helmchen C, Rambold H, Fuhry L, Büttner U. Deficits in vertical and torsional eye movements after uni- and bilateral muscimol inactivation of the interstitial nucleus of Cajal of the alert monkey. Exp Brain Res. 1998;119:436–452.
20. Büttner U, Büttner-Ennever JA, Rambold H, Helmchen C. The contribution of midbrain circuits in the control of gaze. Ann N Y Acad Sci. 2002;956:99–110.
21. Averbuch-Heller L, Zivotofsky AZ, Das VE, DiScenna AO, Leigh RJ. Investigations of the pathogenesis of acquired pendular nystagmus. Brain. 1995;118:369–378.
22. Bowen M, Peragallo JH, Kralik SF, et al. Magnetic resonance imaging findings in children with spasmus nutans. J AAPOS. 2017;21:127–130.
23. Payne JM, Pickering T, Porter M, et al. Longitudinal assessment of cognition and T2-hyperintensities in NF1: an 18-year study. Am J Med Genet A. 2014;164A:661–665.
24. Billiet T, Mädler B, D'Arco F, et al. Characterizing the microstructural basis of "unidentified bright objects" in neurofibromatosis type 1: a combined in vivo multicomponent T2 relaxation and multi-shell diffusion MRI analysis. Neuroimage Clin. 2014;4:649–658.